19th Australasian Fluid Mechanics Conference
Melbourne, Australia
8-11 December 2014

PLIF Temperature Imaging of a Mach 9 Blunt Body

D. Estruch-Samper[1,2], L. Vanstone[1], B. Ganapathisubramani[3] and R. Hillier[1]

[1] Department of Aeronautics
Imperial College London, SW7 2AZ, United Kingdom

[2] Department of Mechanical Engineering
National University of Singapore, 117575, Singapore

[3] Engineering and the Environment
University of Southampton, SO17 1BJ, United Kingdom

Abstract

Experimental investigation plays a key role in the design of hypersonic vehicles, which generally involve blunt geometries associated to complex flows with high entropy regions and sharp temperature gradients. The present work is concerned with the application of a planar laser-induced fluorescence (PLIF) diagnostic in a hypersonic gun tunnel at Mach 9 nominal freestream conditions. Toluene is used as a tracer given its relatively high frequency quantum yield for short periods and temperature-dependent fluorescence when excited by a UV laser, with a wavelength of 266 nm in the present tests. This novel technique is validated for flow thermometry applications in hypersonic nitrogen-driven facilities, where oxygen quenching effects are avoided thus facilitating the quantitative measurement of temperature within a plane in the flow. To this end, experimental measurements of planar temperature contours around a hypersonic blunt body are presented.

Introduction

While temperature is one of the main parameters of interest in hypersonic flows, its measurement in wind tunnel experiments has traditionally relied on surface-mounted instrumentation [14]. Optical diagnostics may also offer the capabilities to perform non-intrusive measurements within the flow but their application has proven to be particularly difficult in hypersonic facilities, where optical access is restricted and the extreme pressures and strong flow gradients, together with the inherently short test durations and fast flow speeds, pose particular challenges [3].

Planar laser-induced fluorescence (PLIF) is a family of optical diagnostics that has gained importance in recent years. PLIF methods rely on probing the fluorescence of a trace species, either already present or purposely introduced in the flow, following excitation by laser light. Through calibration of the related photo-physical properties, information from the flow can be obtained, which may vary depending on the nature of the study and the actual variance of the technique. PLIF methods have particularly received attention in propulsion and combustion research for the measurement of species concentrations, often occurring naturally in combustion products, for example using hydroxyl radical (OH) and nitric oxide (NO) as the trace species [1, 15]. A number of PLIF variances have been applied in high-speed wind tunnel testing to date including OH PLIF – used for flow visualisation in a supersonic combustion facility [8], krypton PLIF – for scalar imaging in a supersonic underexpanded jet [12], acetone PLIF – for measuring density distribution within a supersonic free jet [6], and NO PLIF – for application in facilities where NO is naturally occurring such as in arc-heated tunnels [13, 7], amongst a few others. Recent research has highlighted the potential of using toluene as a PLIF tracer for flow thermography applications given its strong temperature dependence [9, 10, 16, 11]. The present paper presents an investigation on the applicability of the toluene PLIF technique in hypersonic flows.

Experimental Approach

Imperial College Gun Tunnel

The facility used for the present purposes is the Imperial College gun tunnel, which uses nitrogen as the test gas and makes use of a contoured nozzle to produce a free stream Mach number of $M_\infty \approx 9$ with a test duration of about 25 ms with a established flow time of 6 ms. The Reynolds number for the present experiments was Re_∞= 47.4x10^6 m^{-1} and wall temperature was at ambient conditions T_w = 293 K $\pm$1.5%, while the nominal isentropic free stream temperature and pressure were $T_\infty = 68.3K$ and $p_\infty = 3100Pa$ (Table 1). These low values are a result of the high Mach number of the flow and they are in much contrast to the extremely high stagnation properties which are respectively two and four orders of magnitude higher ($T_{0,\infty}$ = 1150K and $p_{0,\infty}$ = 60.8MPa).

Free stream flow conditions	
M_∞	8.9 $\pm$0.5%
$P_{0,\infty}$ (MPa)	60.8 $\pm$2%
$T_{0,\infty}$ (K)	1150 $\pm$4%
Re_∞ (m^{-1})	47.4 x 10^6 $\pm$7%

Table 1: Free stream flow properties for present tests at Imperial College gun tunnel.

Test Set-up

The test model consisted of a blunt cylinder with a spherical nose of radius 25 mm (Fig. 1a) [4]. The laser-sheet forming optics included a biconvex lens (25.4mm-diameter and 550 mm focal length) and a round cylindrical plano-concave lens (15mm-diameter, 25mm focal length) as well as a set of round mirrors, all of them made of fused silica and with 248 - 355 nm anti-reflective coating. An intensified CCD camera (Princeton Instruments, 512 x 512 pixels, Gen II with P43 phosphor plate) was externally triggered and gated for the duration of the established flow run, with no hardware binning; a UV camera lens kit (Nikon, UV-105mm) was used to image a field of view of 77.95 mm x 77.95 mm with a resolution of 3.271px/mm. An Nd:YAG laser with 266 nm excitation was triggered using the start of the run as a reference and timed to excite the flow at the middle of the established flow window (i.e. 13 ms from trigger) following the ramp-up to steady test conditions and prior to the subsequent ramp-down (Fig. 1b). Spectrophotometric grade toluene with high purity was used (Sigma Aldrich) and the mixture was set with a molar mass concentration of 1.0%

(a)

(b)

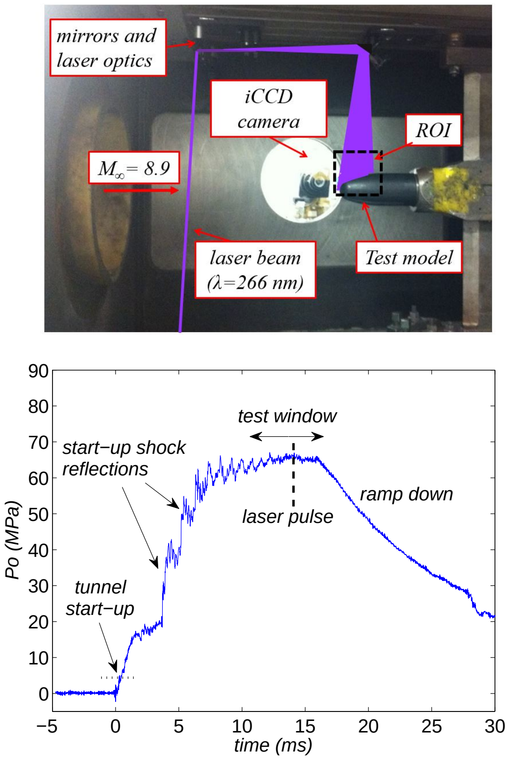

Figure 1: Photograph of experimental rig indicating region of interest (ROI) *(a)* and gun tunnel total pressure trace indicating different stages of an individual run *(b)*.

of toluene in nitrogen, corresponding to a toluene partial pressure of 4 mbar, which proved to yield sufficiently high signal intensities within the temperature range of interest and is well below the saturation pressure of toluene ($\sim$ 50 mbar at ambient temperature).

PLIF Method

The toluene PLIF diagnostic relies in the correlation between the fluorescence characteristics of toluene and the amount of oxygen and temperature of the flow under a certain range of conditions of relevance to the experiments. In mixtures free of oxygen, such as in the present application, the photo-physical characterisation of toluene fluorescence can be simplified so that quenching effects are avoided and the LIF signal (S_{LIF}) therefore becomes a function of the incident number of photons $\frac{E}{h\nu}$ (where E is the fluence of the excitation laser, h is Planck's constant and ν is the frequency of the excitation laser), the fraction of photons absorbed $n_{tol}\sigma$ (which is the number density of fluorescing species, $n_{tol} = P_{tol}/(RT)$, times the absorption cross section, σ), the fraction of photons re-emitted as fluorescence ϕ (or FQY), and the overall efficiency of the imaging system η. While the absorption cross section is a function of excitation wavelength and temperature $\sigma(\lambda_{ex}, T)$ and the efficiency of the system is a function of the fluorescence wavelength, $\eta(\lambda)$, the FQY (or ϕ) of toluene is a function of the particular wavelength at which toluene fluoresces and at which it is excited, λ and λ_{ex}, as well as a function of the flow temperature and pressure, and tracer partial pressure, T, P and P_{tol}. For a given mixture, excitation wavelength and spectral filter combination, the PLIF image obtained can thus be expressed as follows, where (x,y) are the spatial locations corresponding to each pixel in the horizontal and vertical directions in the image:

$$S_{LIF}(x,y,T) = E(x,y)n_{tol}(x,y)\sigma(x,y)\phi(T(x,y))\eta \qquad (1)$$

This relation permits application to constant pressure flows with homogeneous tracer distributions by means of a single-band approach but the assumptions above do not apply to flows involving pressure changes and therefore with non-uniform tracer distributions. In such cases, a two-colour approach can be used, which relies in imaging the flow field using two different spectral filters, each of them imaging a different portion of the fluorescence spectrum. The filters are usually referred to as *red* and *blue* based on the part of the fluorescence spectrum they transmit, i.e. imaging of the higher wavelengths corresponds to the *red* filter and the lower wavelengths corresponds to the *blue* filter. After taking into account the efficiency of the filters for a particular imaging system, which is also a function of wavelength $\eta(\lambda)$ (including camera quantum efficiency, overall transmission of the optics, etc.), the ratio of the two corresponding signal intensities, S_{red} and S_{blue}, can be expressed as follows:

$$\frac{S_{red}}{S_{blue}} = \frac{E(x,y)n_{tol}(x,y)\sigma(T(x,y))\phi(T(x,y))_{red}}{E(x,y)n_{tol}(x,y)\sigma(T(x,y))\phi(T(x,y))_{blue}} \qquad (2)$$

Therefore, by calculating the ratio between the two images, most of the variables cancel each other and the LIF signal at a given pixel in the image becomes a function of the ratio of FQY captured by each filter thus allowing to measure temperature within the imaged plane:

$$\frac{S_{red}(x,y,T)}{S_{blue}(x,y,T)} = cnt\,\frac{\phi(T(x,y))_{red}}{\phi(T(x,y))_{blue}} \qquad (3)$$

The fully steady and highly repeatable flow in the present test case, as established in past experiments by means of thin-film heat transfer measurements and high-speed schlieren visualisation [4], allowed using a one-camera set-up for which the spectral filter was changed between runs. Given the short run durations (6 ms) and the low laser frequency (15 Hz), a single image per tunnel firing was obtained and 3 repeat runs were performed per filter as a proof-of-concept approach.

Toluene Spectroscopy

An intensified CCD (iCCD) spectrometer was used (Princeton Instruments iCCD, 600 line mm^{-1} grating) to obtain spectral measurements within the 265 to 322 nm range. The spectral profiles exhibit two peaks at 277 nm and 282 nm, as well as the 266 nm peak which corresponds to the excitation wavelength and proved to be pressure-independent except near the excitation wavelength (266 nm), where Rayleigh scattering effects – essentially elastic scattering near the laser wavelength – result in a peak that increases in intensity and broadens across the spectral range as pressure is decreased, below about 500mbar, artificially increasing signal intensity by up to around 10% near vacuum conditions ($\sim$ 10 mbar).

The dependence on temperature was subsequently investigated by heating up the mixture and the insulated test cell to 380 K. As shown in Figure 2, this increase in temperature results in a red shift of the fluorescence spectral profile of approximately 2-3 nm with respect to the spectral profile at ambient conditions ($T_{amb} = 293K \pm 1.5$), with the shift being more noticeable towards the upper half of the profile ($> 282nm$) and the lower side being less sensitive to temperature. A band-pass filter of the type BP280 (Semrock FF01-280/20-25), centred at 280nm with a nominal band pass of 280 ± 10 nm, was used to image the left side of the profile (*blue* filter) and a long-pass filter (Schott N-WG280) with cut-off at about 280nm was used to capture the right side of the profile (*red* filter). Given the demonstrated high linearity of the PLIF signal for temperatures up to 500 K [9], it appears reasonable to assume the same linear trend may

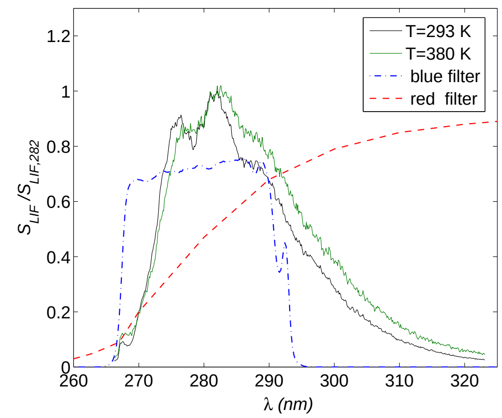

Figure 2: Toluene fluorescence spectra at atmospheric conditions, T=293 K, and at a temperature of 380 K with corresponding shift in the spectral profile, normalised by intensity at 282 nm, and indicating manufacturer-provided filter curves.

be maintained for the lower temperatures. In this manner, following calibration of the system efficiency response, correction for background and dark noise signal based on standard pre-test image subtraction and application of a 4x4 spatial filter, the images were eventually correlated to temperature.

Experimental Results

Raw PLIF data are presented in Figures 3a and b, which correspond respectively to the *blue* and *red* images. In both of them, the location of a bow shock ahead of the nose can be distinguished, with higher contrast across the shock in the *red* image (note that the intensity of the *red* image in Figure 3b has been increased to approximately match the intensity in the downstream for better clarity). In both cases, the higher density and temperature downstream of the shock wave results in an increase in intensity through it, which is partly due to the higher pressure downstream of the shock, and hence higher toluene density.

Following post-processing of the image pair, the distribution of temperature around the blunt nose is obtained as presented in Figure 4a on a colour scale, with lower temperatures shown in blue colour and higher temperatures in red as per the legend. The corresponding locations of the camera field of view (FOV) and the laser sheet are indicated in the schlieren image in Figure 4b. Following extensive attempts to capture the flow at the immediate start of the nose, it was concluded that measurements could not be accurately obtained further upstream of the selected region ($x < 15mm$), partly as a result of the high temperatures in the stagnation region exceeding the pyrolisis temperature of toluene from about 900 K [2], where the stagnation point temperture is $T_o = 1150$ K, and also due to the relatively low signal intensities at high temperatures and the limitation to use a relatively low concentration of toluene for the present tests.

Repeatability in terms of ratios across the shock is found to be within $\pm 1\%$. In terms of overall intensity, a higher uncertainty (5%) related to variation in the laser excitation energy is found, mainly due to the variation in tunnel start-up (which relies on the rupture of two diaphragms and varies depending on the material and corresponding machining) thus resulting in different laser warm-up times. The free stream pressure is analytically calculated from isentropic relations and it is found to be 31 mbar (which is the lowest pressure within the flow); the pressure in

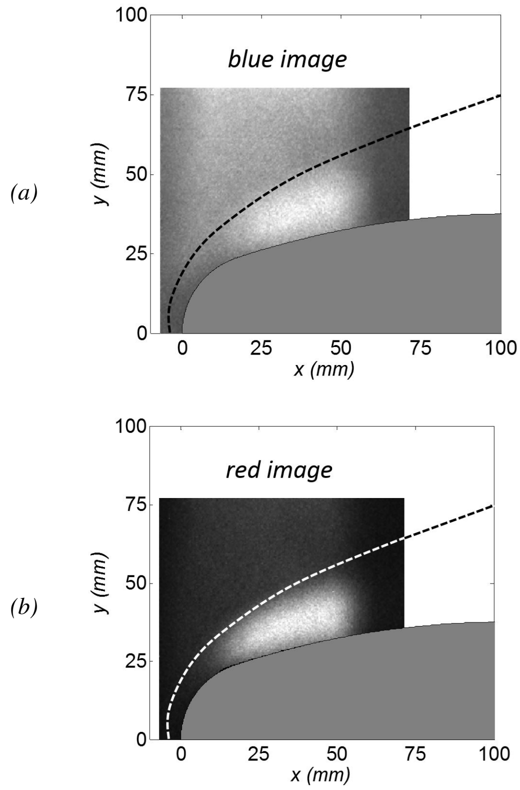

Figure 3: Raw PLIF images on hypersonic blunt nose: *blue* image *(a)* and *red* image *(b)*. Relative intensity of *red* image increased $\times 3$ times for presentation purposes.

the region of interest downstream of the shock is significantly higher ($\sim 250 mbar$ based on the numerical simulations) so that Rayleigh scattering is expected to be relatively low. Based on the corrections developed during calibration, Rayleigh effects are expected to account for 11.6% and 2.6% of the total intensity of the image in these two regions.

Taking into account the different uncertainties that have been mentioned, the total measurement error at near ambient conditions is found to be of 15%, including a 2% error related to laser profile, 5% due to uncertainties regarding excitation energy, and an 8% related to calibration of the signal ratio for the filter pair (the latter including spectrometer, iCCD imaging, and temperature measurement uncertainties). Prior to application of the Rayleigh scattering corrections, the error would be 10% higher, i.e. with a total of 25%.

Conclusions

The applicability of the toluene PLIF technique for imaging of flow temperature in hypersonic low-enthalpy facilities has been assessed. The main appeal of using toluene as a tracer is its strong temperature dependence and high FQY, which make it particularly suitable for thermometry applications in oxygen-free environments. 266 nm excitation provides relatively high FQY but the proximity of this wavelength to the toluene emission spectra results in elastic scattering effects that are difficult to be blocked sharply without altering the results obtained with the *red*-to-*blue* filter combination. However, Rayleigh scattering contamination is of the order of 10% at the lowest pressure conditions and can be taken into account with the appropriate corrections. High temperatures occurring in stagnation regions

(a)

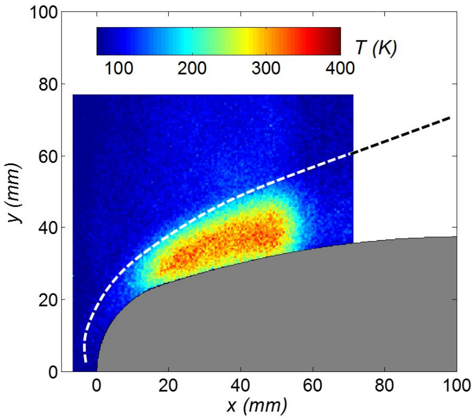

(b)

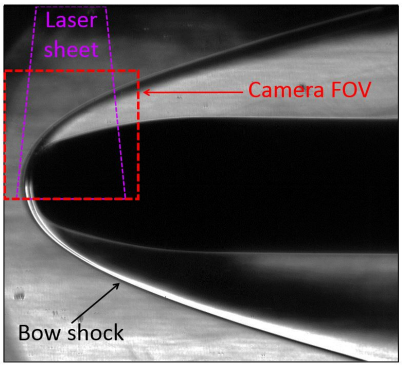

Figure 4: Toluene PLIF results on hypersonic blunt nose *(a)* and corresponding schlieren visualisation indicating location of laser sheet, camera field of view (FOV) *(b)*.

in high Mach number flows are outside the range of the technique due to toluene pyrolysis effects and to reduced FQYs, however, larger amounts of toluene could yield measurements in regions with temperatures as high as 900 K.

The technique thus offers the potential of yielding measurements of planar temperature distributions around hypersonic bodies, in which this property is particularly of high importance but yet the majority of investigations to date have been limited to obtaining surface measurements.

Acknowledgements

This work was carried out under the Engineering and Physical Sciences Research council (EPSRC) grant EP/H020853/1 and made use of the EPSRC Engineering instrument Pool to borrow the iCCD spectrometer and iCCD imaging camera.

References

[1] Cessou, A., Meier, U. & Stepowski, D. Applications of Planar Laser Induced Fluorescence in Turbulent Reacting Flows. *Meas. Sci. Technol.*, **11**(7), 2000, 887-901.

[2] D'Alessio, J., Lazzaro, M., Massoli, P. & Moccia, V. Absorption Spectroscopy of Toluene Pyrolysis. *Opt. Las. Eng.*, **37**, 2002, 495-508.

[3] Estruch-Samper, D., Lawson, N. & Garry, K. Application of Optical Measurement Techniques to Supersonic and Hypersonic Aerospace Flows. *J. Aerosp. Eng.*, **22**(4), 2009, 383-395.

[4] Estruch-Samper, D., Vanstone, L., Ganapathisubramani, B. & Hillier, R. Effect of Roughness-Induced Disturbances on Axisymmetric Hypersonic Laminar Boundary Layer. AIAA paper 2012-675, 2012.

[5] Faust, S., Dreier, T. & Schulz, C. Temperature and Bath Gas Composition Dependence of Effective Fluorescence Lifetimes of Toluene Excited at 266 nm. *Chem. Phys.*, **383**(13), 2011, 611.

[6] Hatanaka, K., Saito, T., Hirota, M., Nakamura, Y., Suzuki, Y. & Koyaguchi, T. Flow Visualization of Supersonic Free Jet Utilizing Acetone PLIF. *Vis. Mech. Proc.*, **2**(1), 2012.

[7] Inman, J.A., Bathel, B.F., Johansen, C.T., Danehy, P.M., Jones, S.B., Gragg, J.G. & Splinter, S.C. Nitric Oxide PLIF Measurements in the Hypersonic Materials Environmental Test System (HYMETS). At the 49th AIAA Aerospace Sciences Meeting, AIAA paper 2011-1090, 2011.

[8] Johansen, C.T., McRae, C.D., Daney, P.M., Gallo, E.C.A., Cantu, L.M.L., Magnotti, G., Cutler, A.D., Rockwell Jr, R.D., Goyne, C.P. & McDaniel, J.C. OH PLIF Visualization of the UVa Supersonic Combustion Experiment: Configuration A. *J. Vis.*, **17**(2), 2014, 131-141.

[9] Koban, W., Koch, J.D., Hanson, R.K. & Schulz, C. Absorption and Fluorescence of Toluene Vapor at Elevated Temperatures. *Phys. Chem. Chem. Phys.*, **6**(11), 2004, 2940-2945.

[10] Luong, M., Koban, W. & Schulz, C. Novel Strategies for Imaging Temperature Distribution using Toluene LIF. *J. Phys Conf. Ser.*, **45**, 2006, 133-139.

[11] Miller, A.V., Gamba, M., Mungal, M.G. & Hanson, R.K. Single- and Dual-Band Collection Toluene PLIF Thermometry in Supersonic Flows. *Exp. Fluids*, **54**:1539, 2013, 13pp.

[12] Narayanaswamy, V., Burns, R. & Clemens, N.T. Kr-PLIF for Scalar Imaging in Supersonic Flows. *Opt. Lett.*, **36**(21):4185-7, 2011.

[13] O'Byrne, S., Danehy, P.M. & Houwing, A.F.P. Investigation of Hypersonic Nozzle Flow Uniformity using NO Fluorescence, *Shock Waves*, **5**, 2006, 1-7.

[14] Schultz, D.L. & Jones, T.V. Heat–Transfer Measurements in Short–Duration Hypersonic Facilities. *AGARDograph*, **165**, 1973.

[15] Sjoholm, J., Rosell, J., Li, B., Richter, M., Li, Z., Bai, X. & Alden, M. Simultaneous Visualization of OH, CH, CH_2O and Toluene PLIF in a Methane Jet Flame with Varying Degrees of Turbulence. *Proc. Comb. Inst.*, **34**(1), 2012, 1475-1482.

[16] Yoo, J., Mitchell, D., Davidson, D.F. & Hanson, R.K. Near-Wall Imaging using Toluene-based Planar Laser-Induced Fluorescence in Shock Tube Flow. *Shock Waves*, **21**(6), 2011, 523-532.